

RESPONSE OF RC COLUMN TO HORIZONTAL BI-DIRECTIONAL DEFLECTION HISTORY

by

Katsuki TAKIGUCHI^I, Seiji KOKUSHO^{II}
Katsumi KOBAYASHI^{III} and Masahiko KIMURA^{IV}

SUMMARY

This is an experimental and analytical study about bi-directional behavior of restoring force responding to relative displacement between the top and the bottom of a reinforced concrete column which is under constant axial force.

A unique loading apparatus was developed for this experiment and twelve specimens were tested. The aseismic performance of a column was estimated by being compared with those of an ideal mechanical model under the same deflection history with respect to hysteresis energy absorption and restoring force.

A bi-directional restoring force model was formulated. The test results were followed by the model quite well.

INTRODUCTION

For reasonable aseismic design of reinforced concrete framed structures it is indispensable to clarify the restoring force characteristics of columns to bi-directional deflection history. Bi-directional behaviors of columns, however, have been grasped only insufficiently. The authors have been studying the bi-directional behaviors of reinforced concrete columns for recent several years.<9><10><11><12>

This paper deals with bi-directional restoring force responding to bi-directional relative displacement between the top and the bottom of a reinforced concrete column which is under constant axial load.

EXPERIMENT

The loading system was developed in order to keep faces of the bottom and the top of the column precisely parallel. The concept of the loading system is almost same as Okada's one.<8> The loading system, the test setup, a link mechanism and a typical specimen are shown in Fig. 1 - Fig. 3 and Photo. 1 - Photo. 2. Twelve tested specimens are listed in Table 1.

When the apparatus was set up, the bottom stub of the specimen was fastened to a horizontal bearing bed and the top stub to a stiff plate with PC bars. The stiff plate was connected to the bed with a newly developed three dimensional linkage mechanism, which permitted the plate translational motion in any direction and restrained it from any rotational movement. Namely, the test column was deformed compulsorily to have an inflection point near the center of it and prohibited from torsional deformation. Axial force was loaded by weights on the stiff plate. Deflection was imposed on the specimen through two loading beams by two hydraulic jacks

I Associate Professor, Nagoya Institute of Technology, Nagoya, JAPAN

II Professor, Tokyo Institute of Technology, Tokyo, JAPAN

III Graduate Student, Tokyo Institute of Technology, Tokyo, JAPAN

IV Graduate Student, Nagoya Institute of Technology, Nagoya, JAPAN

installed at the level of the specimen's center, and responding shear force was measured by two load cells. Twelve specimens having 15cm × 15cm cross section and 60cm clear height were tested. Elements varied in the experiment were magnitude of constant axial force, deflection history, arrangement of longitudinal reinforcements and amount of hoops. All specimens were laterally reinforced more than being required from the structural standards of Architectural Institute of Japan. The experiment was successfully executed and the maximum rotation of the stiff plate was only 2.0×10^{-3} rad. <12>

A part of experimental results are shown in Fig. 4 - Fig. 12 and Photo. 3 - Photo. 4. With respect to all specimens, any remarkable unstable behavior was not recognized.

ESTIMATION OF ASEISMIC PERFORMANCE

An ideal mechanical model was designed as shown in Fig. 13. When the model is subjected to uni-directional deflection history, it has so-called bi-linear restoring force characteristics. The relation between restoring force and deflection was formulated using the analogy to the theory of elasticity and plasticity. The concept of plastic potential and Ziegler's hardening rule <1><2> were employed, however, anisotropy was considered both in elastic and in plastic range.

Yield locus was postulated to be an ellipse in two-dimensional generalized stress plane. Yield surface is described by Ziegler's rule <1><2>

$$F(Q_1 - \alpha_1, Q_2 - \alpha_2) = k^2 = \text{const.} \quad (1)$$

Q_1, Q_2 : restoring force (generalized stress)
in direction-1 and direction-2
 α_1, α_2 : parameters of kinematic hardening

From the theory of plastic potential with considering orthotropic hardening,

$$[\tilde{w}] \{dP^P\} = \{\partial F / \partial Q\} d\lambda, \quad d\lambda > 0 \quad (2)$$

$[\tilde{w}]$: diagonal matrix for orthotropic hardening
 $\{dP^P\}^T = [dD_1^P, dD_2^P]$, $\{\partial F / \partial Q\}^T = [\partial F / \partial Q_1, \partial F / \partial Q_2]$

From Ziegler's hardening rule, <1><2>

$$\{d\alpha\} = \{Q - \alpha\} d\mu, \quad d\mu > 0 \quad (3)$$

$$\{d\sigma\}^T = [d\alpha_1, d\alpha_2], \quad \{Q - \alpha\}^T = [Q_1 - \alpha_1, Q_2 - \alpha_2]$$

From the condition that stress remains on the yield surface in plastic flow,

$$[dQ - d\alpha] \{\partial F / \partial Q\} = 0 \quad (4)$$

Substituting Eq. 3 into Eq. 4,

$$d\mu = \frac{[\partial F / \partial Q] \{dQ\}}{[Q - \alpha] \{\partial F / \partial Q\}} \quad (5)$$

Assuming that the vector $\{\partial F / \partial Q\}$ is orthogonal to

the vector $\{dQ\} - [w] \{dD^P\}$,

$$[\partial F / \partial Q] (\{dQ\} - [w] \{dD^P\}) = 0 \quad (6)$$

Substituting Eq. 2 into Eq. 6,

$$d\lambda = \frac{[\partial F / \partial Q] \{dQ\}}{[\partial F / \partial Q] [\partial F / \partial Q]} \quad (7)$$

Substituting Eq. 7 into Eq. 2,

$$\{dD^P\} = \frac{[w]^{-1} [\partial F / \partial Q] [\partial F / \partial Q] \{dQ\}}{[\partial F / \partial Q] [\partial F / \partial Q]} \quad (8)$$

In this case, the yield locus is an ellipse, so $w(1,1) = E_1^P$ and $w(2,2) = E_2^P$. From Fig. 13, $1/(E_1^e/100) = 1/E_1^{eP} = 1/E_1^e + 1/E_1^P$ and $1/(E_2^e/100) = 1/E_2^{eP} = 1/E_2^e + 1/E_2^P$. When $d\lambda < 0$, $\{dD^P\} = 0$. As for the elasticity, $\{dD^e\} = [-E^e]^{-1} \{dQ\}$, where $E^e(1,1) = E_1^e$ and $E^e(2,2) = E_2^e$. Total generalized strain (deformation) is represented by $\{dD\} = \{dD^e\} + \{dD^P\}$.

Thus, restoring force responding to deflection history of the ideal model was formulated. E_1^e , E_2^e and initial yield ellipse of the model were determined by referring to ACI-Code.^{<4>}

Hysteresis energy absorption ratio of the tested specimen to the corresponding ideal model $AER = (\int P_1 \cdot d\delta_1 + \int P_2 \cdot d\delta_2) / (\int Q_1 \cdot dD_1 + \int Q_2 \cdot dD_2)$ was computed and it was related to \bar{D}^P , where $\bar{D}^P = \Sigma |dD^P| + |dD^P|$ and $D = \delta$. Restoring force ratio of the specimen to the model $QR = P/\bar{Q}$ was also computed and related to \bar{D}^P , where P and \bar{Q} were defined as shown in Fig. 14. Envelope of $QR - \bar{D}^P$ curve were plotted. From $AER - \bar{D}^P$ curve and $QR - \bar{D}^P$ envelope as shown in Fig. 15 and Fig. 16, aseismic performance of the specimen was estimated. It doesn't seem that the aseismic performance of the specimen C79-8-10-6-35-XY1 is remarkably inferior to that of C79-8-10-6-35-X. Fig. 16 shows that the specimens C78-8-10-6-40-XY1, C79-8-10-6-35-XY1 and C79-8-10-7-40-XY1 have almost same aseismic performance.

BI-DIRECTIONAL RESTORING FORCE MODEL

Bi-directional restoring force model was set up as shown in Fig. 17 by the same way as ideal model mentioned above. Almost same approach was performed by Takizawa.^{<7>} Restoring force characteristics under uni-directional deflection is similar to Fukada's model^{<3>} and Nomura's one.^{<6>} cP , yP and $y\delta$ in Fig. 17 were determined by Sugano's equation.^{<5>}

Some results obtained by this model are shown in Fig. 18, Fig. 19 and Fig. 20, together with experimental results. These figures show that the model can follow the experimental results quite well.

CONCLUSION

The following conclusions were obtained by this study about bi-directional restoring force responding to bi-directional relative displacement between the top and the bottom of a reinforced concrete column under constant axial load.

1. The newly developed loading apparatus is efficient enough.
2. Fundamental data of the twelve specimens were obtained by this experiment.

3. Aseismic performance of a column can be estimated by the proposed method.
4. The columns sufficiently reinforced by hoops have stable restoring force characteristics.
5. The restoring force model formulated here can follow the experimental results quite well.

More and more experiments should be carried out under many varieties of conditions, that is, shear span ratio, axial load, reinforcement ratio, deflection history and so on, admittedly, to generalize the above conclusions.

ACKNOWLEDGEMENT

This study received the grant in aid for scientific research from the Ministry of Education, Science and Culture of Japan. The authors wish to thank the Ministry.

REFERENCES

- 1) Shield, R.T. and Ziegler, H.: 1958: On Prager's Hardening Rule: ZAMP, Vol. IXa, pp. 260-276
- 2) Ziegler, H.: 1959: A Modification of Prager's Hardening Rule: Quart. Appl. Math., Vol. XVII, No. 1, pp. 55-65
- 3) Fukada, Y.: 1969: Study on the Restoring Force Characteristics of R.C. Buildings: Proc. 40th Kanto District Symposium, Architectural Institute of Japan (AIJ), pp. 121-124
- 4) ACI Committee 318: 1970: Proposed Revision of ACI 318-63 Building Code Requirements for Reinforced Concrete (CHAPTER 10 - FLEXURE AND AXIAL LOADS): ACI Journal, Vol. 67, No. 2, pp. 77-146
- 5) Sugano, S. and Koreishi, I.: 1974: An Empirical Evaluation of Inelastic Behavior of Structural Elements in Reinforced Concrete Frames Subjected to Lateral Forces: Proc. V WCEE, Vol. 1, pp. 841-844
- 6) Nomura, S. and Sato, K.: 1976: The Influence of Restoring Force Model on Earthquake Response of R/C Structures: Trans. AIJ Extra, pp. 1273-1276
- 7) Takizawa, H. and Aoyama, H.: 1976: Biaxial Effect in Modeling Earthquake Response of R/C Structures: Earthquake Engineering and Structural Dynamics, Vol. 4, pp. 523-552
- 8) Okada, T., Seki, M. and Asai, S.: 1977: Response of Reinforced Concrete Columns to Bi-Directional Horizontal Force and Constant Axial Force: SEISAN-KENKYU, Monthly Journal of Institute of Industrial Science, University of Tokyo, Vol. 29, No. 5, pp. 48-52
- 9) Takiguchi, K., Kokusho, S. and Okada, K.: 1975 and 1976: Experiments on Reinforced Concrete Columns Subjected to Bi-Axial Bending Moments, Part I and Part II: Trans. AIJ, No. 229 and No. 247, pp. 25-33 and pp. 37-43
- 10) Takiguchi, K., Kokusho, S. and Kobayashi, K.: 1976: Analysis of Reinforced Concrete Sections Subjected to Bi-Axial Bending Moments: Trans. AIJ, No. 250, pp. 1-8
- 11) Kobayashi, K., Kokusho, S. and Takiguchi, K.: 1979: Inelastic Behavior of Reinforced Concrete Members Subjected to Bi-Axial Bending Moments: Proc. AICAP-CEB Symposium, Vol. 2, pp. 141-148
- 12) Takiguchi, K., Kokusho, S., Kobayashi, K. and Kimura, M.: 1979: Study on the Restoring Force Characteristics of Reinforced Concrete Columns to Bi-directional Displacements: Trans. AIJ, No. 286, pp. 29-35

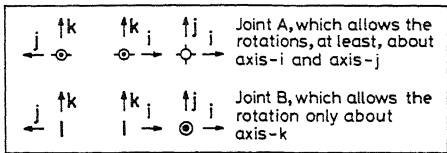
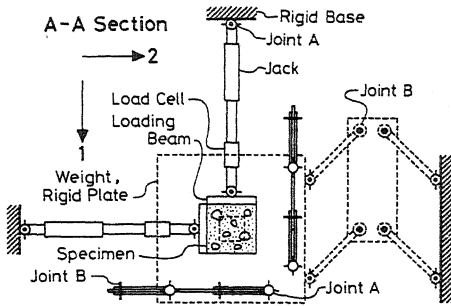
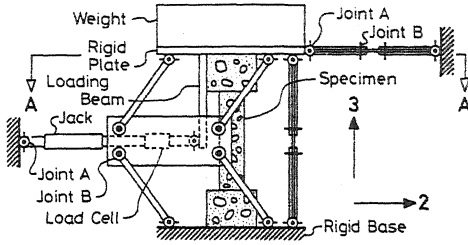


Fig. 1 Loadind System

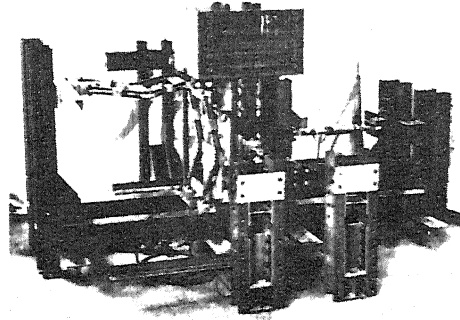


Photo. 1 Test Setup

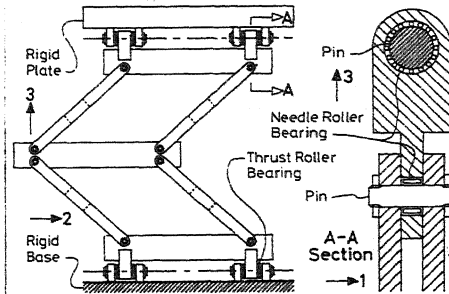


Fig. 2 A link Mechanism

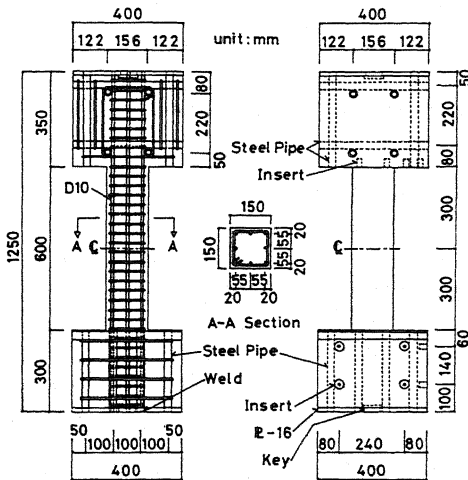


Fig. 3 A typical Specimen

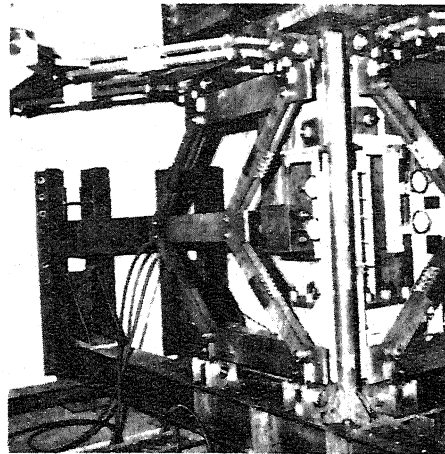


Photo. 2 A Link Mechanism

Table 1 List of Specimens

Test Specimens	Deflection History	Lateral Reinforcement			Longitudinal Reinforcement			Concrete Compressive Strength f_c (kg/cm ²)	N/B-D (kg/cm ²)	Shear Span Ratio
		Size and Interval	Yield Strength (kg/cm ²)	P_w (%)	Number and Size	Yield Strength (kg/cm ²)	P_y (%)			
BBS-0	Uni-Dir.	6 ϕ - 40mm	4368 ^u	0.93	8-D10	3785	2.53	266	4.0	2.0
BBS-1	Bi-Dir. A									
BBS-2	Bi-Dir. B									
C78-8-10-6-40-X	Uni-Dir.	6 ϕ - 35mm	2595	1.07	8-D10	3723	2.53	303	28.5	2.0
C78-8-10-6-40-XY1	Bi-Dir. A									
C79-8-10-6-35-X	Uni-Dir.									
C79-8-10-6-35-XY1	Bi-Dir. A	7 ϕ - 40mm	4447 ^u	1.28	8-D10	3723	2.53	303	28.5	2.0
C79-8-10-7-40-X	Uni-Dir.									
C79-8-10-7-40-XY1	Bi-Dir. A									
C79-6-10-6-35-X	Uni-Dir.	6 ϕ - 35mm	2595	1.07	6-D10	3723	1.90	303	28.5	2.0
C79-6-10-6-35-Y	Uni-Dir.									
C79-6-10-6-35-XY1	Bi-Dir. A									

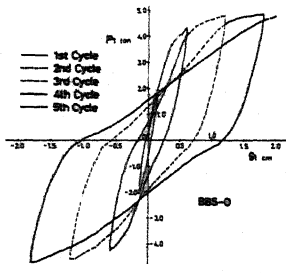


Fig. 4 $P_1-\delta_1$ Curve

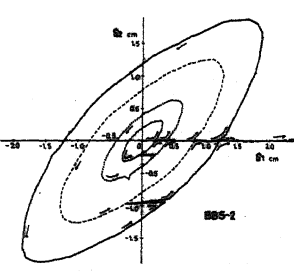


Fig. 5 $\delta_1-\delta_2, P_1-P_2$ Curves

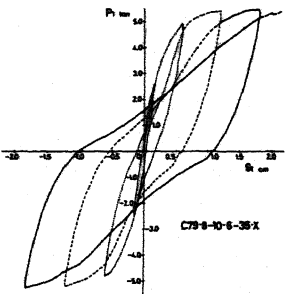
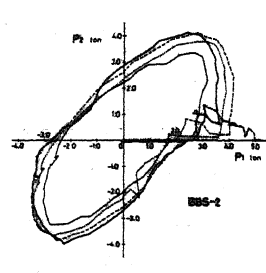


Fig. 6 $P_1-\delta_1$ Curve

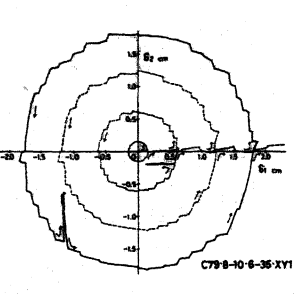
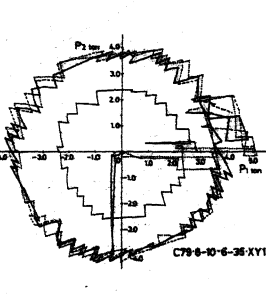


Fig. 7 $\delta_1-\delta_2, P_1-P_2$ Curves



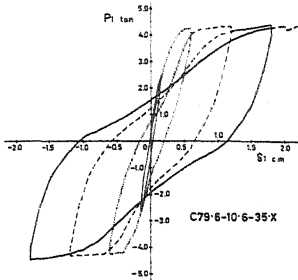


Fig. 8 $P_1-\delta_1$ Curve

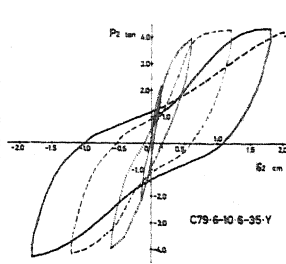


Fig. 9 $P_2-\delta_2$ Curve

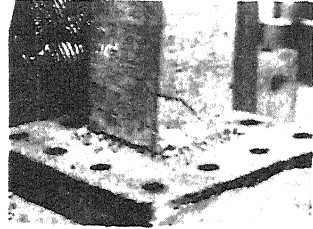


Photo. 4 Lower Part of C79-6-10-6-35-X after Experiment

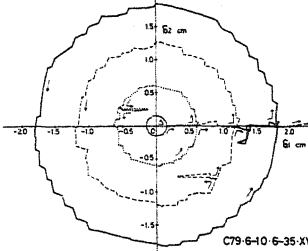


Fig. 10 $\delta_1-\delta_2, P_1-P_2$ Curves

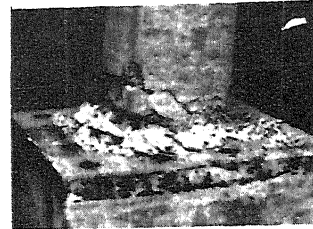
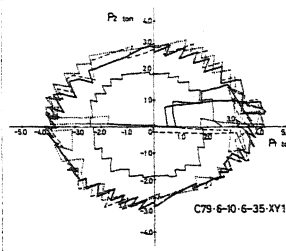


Photo. 4 Lower Part of C79-6-10-6-35-XY1 after Experiment

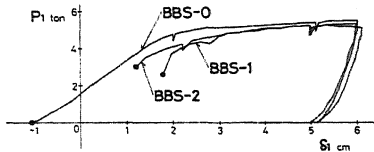


Fig. 11 $P_1-\delta_1$ Curves in the Last Cycle of Loading

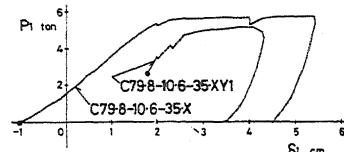


Fig. 12 $P_1-\delta_1$ Curves in the Last Cycle of Loading

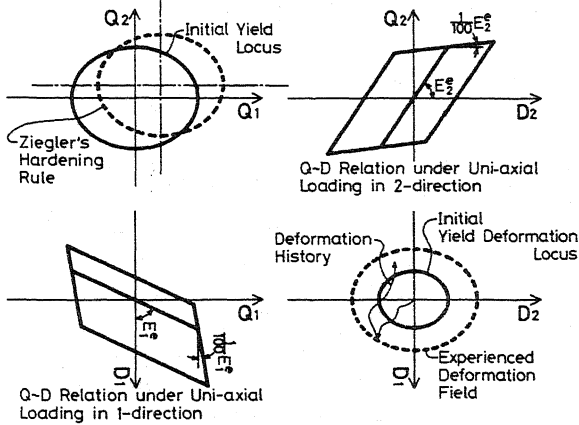


Fig. 13 Ideal Mechanical Model

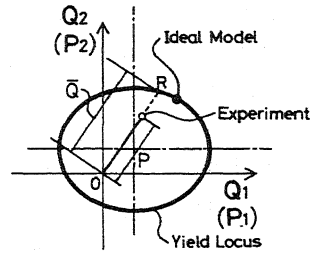


Fig. 14 Illustration of \bar{Q} and P

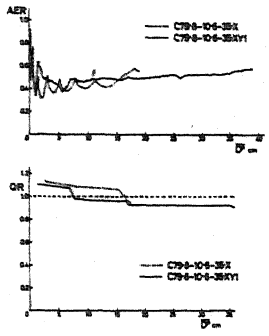


Fig. 15 AER- \bar{D}^P Curves and QR- \bar{D}^P Envelopes

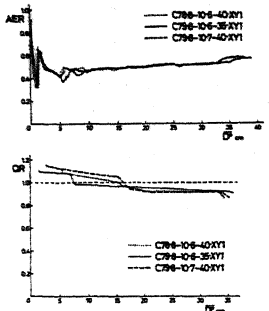


Fig. 16 AER- \bar{D}^P Curves and QR- \bar{D}^P Envelopes

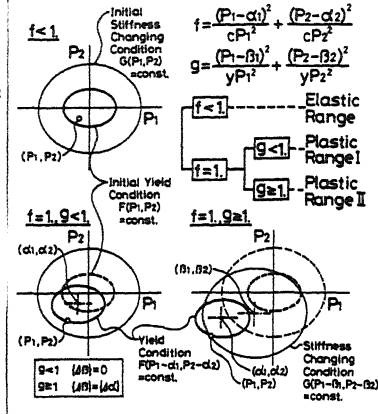
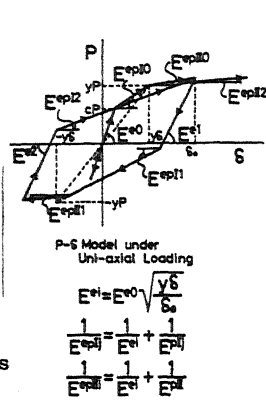


Fig. 17 Two-Dimensional Restoring Force Model

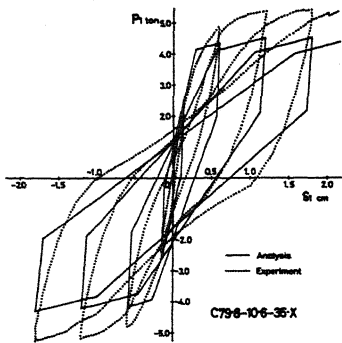


Fig. 18 $P_1 - \delta_1$ Curves

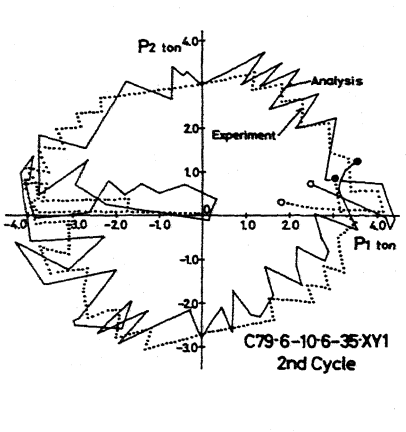


Fig. 19 $P_1 - P_2$ Curves

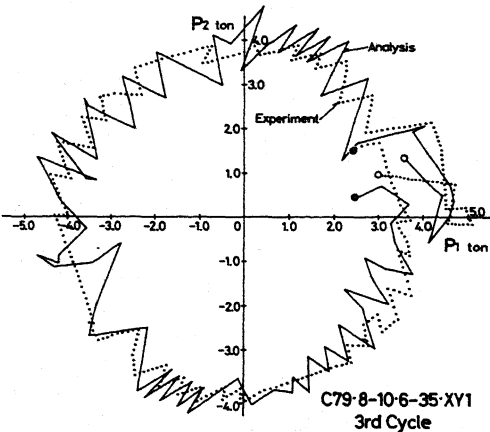


Fig. 20 $P_1 - P_2$ Curves